

## FURTHER RESULTS OF TiO-BAND OBSERVATIONS OF STARSPOTS<sup>1</sup>

DOUGLAS O’NEAL

Department of Physics, Allegheny College, Meadville, PA 16335; doneal@allegheny.edu

JAMES E. NEFF

Department of Physics and Astronomy, College of Charleston, Charleston, SC 29424; neffj@cofc.edu

STEVEN H. SAAR

Harvard-Smithsonian Center for Astrophysics, 60 Garden Street, Cambridge, MA 02138; saar@head-cfa.harvard.edu

AND

MANFRED CUNTZ

Department of Physics, University of Texas, Arlington, TX 76019; cuntz@uta.edu

Received 2003 October 27; accepted 2004 June 17

### ABSTRACT

We present measurements of starspot parameters (temperature and filling factor) on five highly active stars, using absorption bands of TiO, from observations made between 1998 March and 2001 December. We determined starspot parameters by fitting TiO bands using spectra of inactive G and K stars as proxies for the unspotted photospheres of the active stars and spectra of M stars as proxies for the spots. For three evolved RS CVn systems, we find spot filling factors between 0.28 and 0.42 for DM UMa, 0.22 and 0.40 for IN Vir, and 0.31 and 0.35 for XX Tri; these values are similar to those found by other investigators using photometry and Doppler imaging. Among active dwarfs, we measured a lower spot temperature (3350 K) for EQ Vir than found in a previous study of TiO bands, and for EK Dra a lower spot temperature ( $\sim 3800$  K) than found through photometry. For all active stars but XX Tri, we achieved good phase coverage through a stellar rotational period. We also present our final, extensive grid of spot and nonspot proxy stars.

*Key words:* stars: activity — stars: atmospheres — stars: spots — techniques: spectroscopic

### 1. INTRODUCTION

In previous papers of this series, we described techniques using absorption bands of the titanium oxide (TiO) molecule near 7055 Å [the 7055, 7088, and 7126 Å bands of the  $\gamma(0,0)$  system] and the band at 8860 Å [the strongest of the  $\delta(0,0)$  system] to measure the temperatures and areas of dark, cool starspots in the photospheres of magnetically active stars. We use spectra of inactive M stars to model the spotted regions of active star photospheres and spectra of inactive G and K stars to model the unspotted regions. These proxy spectra are weighted by their relative continuum fluxes and by a surface area filling factor to reproduce spectra of the active stars. The strengths of the two band systems both increase with decreasing temperature (Neff et al. 1995; O’Neal et al. 1996; hereafter Papers I and II, respectively) in stars with  $T_{\text{eff}} \geq 3000$  K but have different temperature sensitivities. Thus, the relative strength of the bands constrains the starspot temperature ( $T_S$ ), while their absolute strengths are functions of the total projected area of starspots on the visible hemisphere (the filling factor  $f_S$ ). The temperature of the nonspotted regions,  $T_Q$ , is usually assumed from the results of previous studies, although it can also be constrained by simultaneous multicolor photometry (if available).

Starspots were discovered by their effect on the photometric light curves of active stars. While multicolor photometry yields valuable information regarding the temperature and total area

of spots (e.g., Strassmeier et al. 1994), it only works if a star has a spot distribution that is highly nonuniform in longitude. In the absence of other data, there are not enough observational constraints provided by one-dimensional light curves to determine the size, shape, and distribution of the spots. A symmetric distribution (either a monolithic polar spot or smaller spots spread evenly in longitude) produces no variation of the star’s brightness. If a star is rotating rapidly, high-resolution spectra obtained at many different rotational phases provide two-dimensional spatial constraints via velocity amplitude information that can be used to map, or “Doppler image,” the surface distribution (e.g., Vogt et al. 1999; Hatzes & Kürster 1999; Strassmeier 2002, and references therein).

Molecular spectroscopy detects spots regardless of their distribution, even on slowly rotating stars. The idea that TiO bands could be used to measure starspot properties was first stated by Vogt (1979) and Ramsey & Nations (1980); Huenemoerder & Ramsey (1987) presented a more quantitative study of the effect of spots on TiO bandheads. Inspired by these pioneering studies, we began a program to use the TiO bands to systematically measure  $f_S$  and  $T_S$  on late-type stars. We selected a group of stars that were previously expected to be spotted (dwarf BY Dra variables and subgiant/giant RS CVn single-lined binaries). We also observed a sample of G and K stars known not to exhibit high levels of magnetic activity to represent the photospheres of the active stars and a sample of M stars to represent the starspots. (A few of the dwarf proxy stars are moderately active; probably the most active,  $\epsilon$  Eri, exhibits a spot coverage of a few percent [Frey et al. 1991] but no measurable TiO band depth.) To investigate the effect of surface gravity, we included both giant and dwarf comparison stars. For a given observation of an active star,

<sup>1</sup> This paper includes data taken at McDonald Observatory of the University of Texas at Austin.

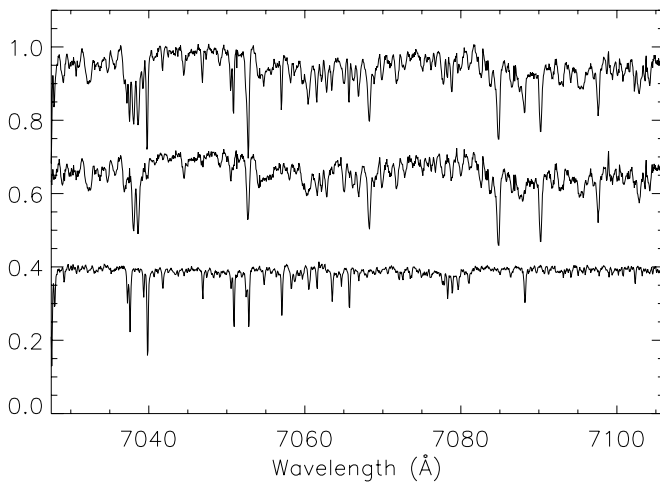


FIG. 1.—Illustration of the “drying” procedure by which telluric lines are removed from active and comparison star spectra. A spectrum of EQ Vir in the region of the 7055 Å TiO bands is shown before (*top*) and after (*middle*) drying. The spectrum of Spica used in the procedure is shown at bottom. All three spectra are normalized and then vertically offset. Differences between the two EQ Vir spectra are seen where there are strong telluric lines in the spectrum of Spica.

we assume that the spot coverage visible at that time can be modeled by a single spot proxy.

We have undertaken several observing runs to obtain additional echelle spectra of active stars, with the following goals: (1) to obtain phase coverage throughout a rotational cycle on several active stars to characterize their starspot properties (good phase coverage gives us information on the longitudinal distribution of starspots), (2) to test the assumption that all spots have the same temperature (O’Neal et al. [1998b, hereafter Paper III] found evidence of multiple spot temperatures on II Pegasi), and (3) to investigate whether chromospheric diagnostics in the visual spectrum correlate with photospheric spot coverage. We present results from observations of five active stars, as well as our final extensive grid of inactive comparison stars.

## 2. OBSERVATIONS AND ANALYSIS

### 2.1. Observations and Data Reduction

The comparison star data were obtained during six observing runs (from 1995 December to 2001 December) with the 2.1 m Otto Struve Telescope at McDonald Observatory, using

the Sandiford Cassegrain Echelle Spectrograph (“CassEchelle”; McCarthy et al. 1993). The active star data presented in this paper were obtained in 1998 March or later. The CassEchelle uses a Reticon  $1200 \times 400$  CCD with  $27 \mu\text{m}$  pixels and yields a resolving power of  $\lambda/\Delta\lambda \approx 60,000$ . Our spectra cover from H $\alpha$  to past the 8860 Å TiO band, with no wavelength gaps shortward of 8500 Å.

We used the REDUCE echelle package (Hall et al. 1994). Bias removal, creation of order maps, flat-field division, scattered light removal, and extraction of the spectra were performed as described by Hall et al. (1994), with two exceptions (which represent departures in our procedure from those used to analyze data presented in previous papers). First, order maps used to extract the spectra were made from the object spectra themselves to lessen the effects of any slight shift in the positions of the orders between object and flat-field spectra. Second, for purposes of scattered light removal, the CCD frames were split in two and the redward orders (where for all but very cool stars the signal was by far the weakest) were reduced separately. For fainter stars, this consistently produced better results in flat-field division and scattered light removal than analyzing the entire frame at once.

For orders containing spectral features of interest, careful normalization was done by fitting a spline to the stellar pseudocontinuum. Telluric lines were removed by the “drying” procedure described in Paper I, using observed spectra of O and B stars. This is particularly important in the regions of H $\alpha$  and the 7055 Å TiO bands, whereas the 8860 Å region is much less affected. This procedure is illustrated in Figure 1, which shows a 7055 Å region spectrum of EQ Vir (from 2000 May 16) along with one of Spica (spectral type B1). The “dried” EQ Vir spectrum (*middle*) is related to the “wet” spectrum (*top*) by  $F_d = F/[1 - (1 - F_{OB})^x]$ . Here,  $F_d$  and  $F$  represent a normalized spectrum of EQ Vir after and before drying, respectively; the value  $F_{OB}$  is the normalized spectrum of the early-type star, containing telluric lines. The parameter  $x$  is adjusted interactively to determine the best fit to the telluric lines in the active star spectrum.

The active stars observed in this program are listed in Table 1. We also list temperature components ( $T_Q$  found by previous studies and  $T_S$  derived in this paper) for each star, as well as the range of  $f_S$  (on different nights of observation) derived from our modeling. Table 2 summarizes our observations of active stars. For each observation, we measured  $f_S$  by the procedure summarized below.

We also measured H $\alpha$  and the Ca II infrared triplet (IRT) emission-line strengths, searching for changes in emission

TABLE 1  
PROPERTIES OF ACTIVE STARS

Name	HD	Spectral Type	$v \sin i$ ( $\text{km s}^{-1}$ )	$P_{\text{rot}}$ (days)	Date <sup>a</sup> ( $\phi = 0$ )	$T_Q^b$ (K)	$T_S$ (K)	$f_S^c$
DM UMa.....	...	K2 III–IV	26	7.4949	47,623.383 <sup>d</sup>	4500	$3450 \pm 126$	0.28–0.42
IN Vir.....	116544	K2–3 IV	24	8.1895	49,422.53 <sup>e</sup>	4600	$3350 \pm 165$	0.22–0.40
XX Tri.....	12545	K0 III	20.8	23.96924	47,814.325 <sup>f</sup>	4750	$3425 \pm 120$	0.31–0.35
EQ Vir.....	118100	K5 Ve	9.5	3.96	<sup>g</sup>	4380	$3350 \pm 115$	0.33–0.45
EK Dra.....	129333	G1.5 V	17.3	2.805	<sup>g</sup>	5830	$\geq 3800$	0.25–0.40

<sup>a</sup> Date = HJD – 2,400,000.

<sup>b</sup> Found by previous studies of the stars; references given in the text.

<sup>c</sup> Minimum and maximum values observed at different rotational phases.

<sup>d</sup> Data from Strassmeier et al. (1993).

<sup>e</sup> Data from Strassmeier (1997).

<sup>f</sup> Data from Strassmeier (1999).

<sup>g</sup> For these two single stars, the time of our first observation in each epoch was defined as  $\phi = 0.0$ .

TABLE 2  
ACTIVE STAR OBSERVATIONS

Date	HJD <sup>a</sup>	$\phi^b$	$f_S$	Exposure Time(s)	S/N at 7055 Å Order
DM UMa:					
1998 Mar 13 .....	50,885.80	0.29	$0.28 \pm 0.06$	3600	100
1998 Mar 14 .....	50,886.84	0.43	$0.34 \pm 0.07$	3600	125
1998 Mar 15 .....	50,887.73	0.54	$0.37 \pm 0.04$	3600	120
1998 Mar 17 .....	50,889.77	0.81	$0.33 \pm 0.06$	3600	90
1998 Mar 18 .....	50,890.71	0.93	$0.28 \pm 0.06$	3600	100
1998 Mar 19 .....	50,891.68	0.07	$0.42 \pm 0.05$	3600	100
IN Vir:					
2000 May 16.....	51,680.75	0.75	$0.22 \pm 0.06$	3600	120
2000 May 18.....	51,682.79	0.99	$0.23 \pm 0.08$	3600	125
2000 May 19.....	51,683.64	0.10	$0.25 \pm 0.08$	3600	110
2000 May 20.....	51,684.75	0.24	$0.33 \pm 0.09$	3600	125
2000 May 21.....	51,685.64	0.34	$0.34 \pm 0.07$	3600	100
2000 May 22.....	51,686.82	0.49	$0.33 \pm 0.06$	3600	120
2000 May 23.....	51,687.65	0.60	$0.22 \pm 0.08$	3600	110
XX Tri:					
2001 Dec 23 .....	52,266.66	0.75	$0.31 \pm 0.05$	3600	140
2001 Dec 24 .....	52,267.71	0.80	$0.35 \pm 0.05$	2400	135
EQ Vir:					
1998 Mar 17 .....	50,889.92	0 <sup>c</sup>	$0.33 \pm 0.08$	2800	120
1998 Mar 18 .....	50,890.88	0.25	$0.47 \pm 0.07$	3600	100
1998 Mar 19 .....	50,891.77	0.48	$0.39 \pm 0.07$	3600	100
2000 May 16.....	51,680.65	0 <sup>c</sup>	$0.39 \pm 0.05$	3600	95
2000 May 18.....	51,682.74	0.53	$0.42 \pm 0.07$	3600	110
2000 May 19.....	51,683.76	0.78	$0.39 \pm 0.06$	3360	100
2000 May 20.....	51,684.62	0.00	$0.34 \pm 0.05$	3600	95
2000 May 21.....	51,685.80	0.29	$0.38 \pm 0.08$	2800	100
2000 May 22.....	51,686.67	0.52	$0.39 \pm 0.07$	3600	110
2000 May 23.....	51,687.70	0.78	$0.45 \pm 0.07$	3600	125
EK Dra:					
2000 May 16.....	51,680.91	0 <sup>c</sup>	$0.27 \pm 0.06$	3600	170
2000 May 18.....	51,682.81	0.68	$0.40 \pm 0.07$	3600	170
2000 May 19.....	51,683.81	0.03	$0.25 \pm 0.05$	3000	165
2000 May 20.....	51,684.84	0.40	$0.30 \pm 0.07$	3600	160
2000 May 21.....	51,685.79	0.74	$0.36 \pm 0.06$	3600	180
2000 May 22.....	51,686.75	0.08	$0.36 \pm 0.05$	3600	180
2000 May 23.....	51,687.79	0.45	$0.31 \pm 0.06$	3600	175

<sup>a</sup> HJD: 2,400,000 + date given.

<sup>b</sup> HJD and phase are given for middle of observation.

<sup>c</sup> For EQ Vir and EK Dra, the time of our first observation is defined as phase 0, as explained in the text.

strengths and profile shapes. To parameterize the strength of emission, we followed the spectral subtraction procedure (e.g., Montes et al. 2000), in which an artificially rotationally broadened spectrum of an inactive star of the same spectral type is subtracted from each active star spectrum. By doing so, we obtain a residual spectrum that contains only the active chromosphere contribution to the emission lines. Montes et al. (1995) discuss this procedure, including its limitations, for the specific case of H $\alpha$ . A comparison star is aligned (corrected for different radial velocities) with the active star via photospheric absorption lines in the two spectra, then subtracted (active minus comparison) to remove the photospheric contribution. Then 1 is added to the subtracted spectrum. Finally, we integrate to find the area within the emission line above the continuum (=1) level. For our purposes, we take emission equivalent widths to be positive.

## 2.2. The Comparison Stars

In Table 3 we list properties of all the inactive comparison stars we have observed with the CassEchelle. A major effort of our observational program was to complete these comparison

grids; they will be useful for future studies of starspot activity. Spectra of these stars are available upon request to the first author. The dividing line between nonspot and spot comparison stars is at  $\sim 4000$  K; while somewhat arbitrary, this is approximately the temperature at which the 7055 Å band becomes strong enough to detect from spectra of heavily spotted stars whose photosphere is too warm for TiO.

Photometry for the comparison stars comes from Stauffer & Hartmann (1986) and the Bright Star Catalogue (Hoffleit & Jaschek 1982). To compute  $T_{\text{eff}}$  values, we used: (1) for M dwarfs, the  $T_{\text{eff}}$  versus  $(R-I)_{\text{KC}}$  relation by Bessell (1991); (2) for G and K dwarfs, the  $T_{\text{eff}}$  versus  $B-V$  relation by Houdashelt et al. (2000a); (3) for M giants, the average of the  $T_{\text{eff}}$  versus  $V-I$  relation by Strassmeier & Schordan (2000) and the  $T_{\text{eff}}$  versus  $V-K$  relations by Houdashelt et al. (2000b) and Bessell et al. (1998); and (4) for G and K giants, the average of the  $T_{\text{eff}}$  versus  $V-I$  relation by Strassmeier & Schordan (2000), the  $T_{\text{eff}}$  versus  $V-K$  relation by Bessell et al. (1998), and the  $T_{\text{eff}}$  versus  $B-V$  relation by Houdashelt et al. (2000b). All  $T_{\text{eff}}$  values were rounded to the nearest interval of 25 K. Several new  $T_{\text{eff}}$  versus color relations have been published in recent years, so some

TABLE 3  
PROPERTIES OF COMPARISON STARS

Name	HD	HR	Sp. Type	$V$	$(B-V)$	$(R-I)$	$(V-K)$	$T_{\text{eff}}$
Subgiant and Giant Comparison Stars								
1 Gem .....	41116	2134	G5 III	4.2	0.82	0.45	2.02	5175
BD +34°1524.....	53329	2660	G8 IV	5.6	0.91	...	...	5050
10 LMi .....	82635	3800	G8 III	4.6	0.92	0.46	...	5025
$\epsilon$ Vir.....	113226	4932	G8 III	2.8	0.94	0.45	2.04	5025
$\kappa$ Gem.....	62345	2985	G8 III	3.6	0.93	0.45	2.11	5000
BD +04°4434.....	194013	7794	G8 III-IV	5.3	0.97	0.50	...	4900
$\delta$ Aur.....	40035	2077	K0 III	3.7	0.99	0.51	2.26	4850
$\kappa$ CrB.....	142091	5901	K1 IV	4.8	1.00	0.49	...	4850
BD -20°2936.....	82734	3808	K0 IV	5.0	1.02	...	2.27	4825
$\delta$ Ari.....	19787	951	K2 III	4.4	1.03	0.51	2.29	4800
$\circ$ Col.....	34642	1743	K0 IV	4.8	1.00	0.55	2.36	4800
$\beta$ Lac.....	212496	8538	G8.5 III	4.4	1.01	0.57	2.37	4775
$\gamma$ Cep.....	222404	8974	K1 IV	3.2	1.03	0.51	2.29	4775
52 Cyg.....	197912	7942	G9.5 III	4.2	1.06	0.53	2.33	4750
$\gamma^2$ Del.....	197964	7948	K1 IV	4.3	1.04	0.48	2.45	4700
$\theta$ Cet.....	8512	402	K0 III	3.6	1.06	0.56	2.41	4700
$\delta$ Cnc.....	74442	3461	K0 III	3.9	1.08	0.54	2.43	4675
$\chi$ Gem.....	66216	3149	K2 III	4.9	1.12	...	...	4600
58 Leo.....	95345	4291	K1 III	4.9	1.16	0.56	...	4525
$\kappa$ Lyr.....	168775	6872	K2 IV	4.3	1.17	0.55	2.60	4500
$\sigma$ Hya.....	73471	3418	K1 III	4.4	1.21	0.56	2.64	4450
$\kappa$ Leo.....	81146	3731	K2 III	4.5	1.23	0.63	2.78	4375
$\rho$ Boo.....	127665	5429	K3 III	3.6	1.30	0.65	2.93	4275
$\nu$ UMa.....	98262	4377	K3 III	3.5	1.40	0.70	3.18	4125
$\beta$ Cnc.....	69267	3249	K4 III	3.5	1.48	0.78	3.40	4025
$\alpha$ Lyn.....	80493	3705	K7 III	3.2	1.55	0.90	3.74	3900
68 Vir.....	116870	5064	K5 III	5.3	1.52	0.87	3.68	3875
$\mu$ UMa.....	89758	4069	M0 III	3.1	1.59	0.96	3.93	3825
$\kappa$ Ser.....	141477	5879	M0.5 III	4.1	1.62	0.98	4.06	3800
2 Peg.....	204724	8225	M1 III	4.6	1.62	1.09	...	3800
DU Lyn.....	62647	2999	M3 III	5.2	1.58	...	4.29	3700
82 Vir.....	119149	5150	M1.5 III	5.0	1.63	1.16	4.36	3705
$\beta$ Peg.....	217906	8775	M2.5 III	2.4	1.67	1.32	4.66	3625
$\delta$ Vir.....	112300	4910	M3 III	3.4	1.58	1.33	4.61	3625
54 Eri.....	29755	1496	M3 III	4.4	1.61	1.38	4.70	3600
$\mu$ Gem.....	44478	2286	M3-4 III	2.9	1.64	1.38	4.74	3600
$\tau^4$ Eri.....	20720	1003	M3-4 III	3.7	1.62	1.46	4.87	3575
TV Psc.....	2411	103	M3 III	5.1	1.65	1.54	5.19	3550
BY Boo.....	123657	5299	M4.5 III	5.3	1.59	1.66	5.62	3500
$\delta^2$ Lyr.....	175588	7139	M4 III	4.3	1.68	1.63	5.63	3500
FS Com.....	113866	4949	M5 III	5.6	1.59	1.81	5.85	3475
R Lyr.....	175865	7157	M5 III	4.2	1.59	1.91	6.12	3450
VY Leo.....	94750	4267	M5.5 III	5.8	1.45	2.09	6.50	3375
RZ Ari.....	18191	867	M6 III	5.9	1.47	2.17	6.98	3300
S Lep.....	41698	2156	M6 III	6.8	1.63	2.37	7.30	3125
R Hya.....	117287	5080	M7 III	6.4	1.60	2.42	7.60	3050
Dwarf Comparison Stars								
Sun .....	...	...	G2 V	...	0.65	...	...	5800
$\kappa$ Cet.....	20630	996	G5 V	4.8	0.68	0.36	...	5600
61 UMa.....	101501	4496	G8 V	5.3	0.74	0.36	1.74	5550
70 Vir.....	117176	5072	G4 V	5.0	0.71	0.39	1.74	5550
$\sigma^2$ Eri.....	26965	1325	K1 V	4.4	0.82	0.45	2.03	5175
BD +21°1528.....	54563	2692	G9 V	6.9	0.89	...	...	5100
$\epsilon$ Eri.....	22049	1084	K2 V	3.7	0.88	0.47	2.03	5050
$\gamma$ Lep B.....	38392	1982	K2 V	6.2	0.94	...	...	4950
Gl 105A.....	16160	753	K3 V	5.8	0.97	0.53	2.38	4775
BD -05°1123.....	32147	1614	K3 V	6.2	1.03	0.49	...	4750
Gl 570A.....	131977	5568	K4 V	5.7	1.11	0.54	2.65	4575
61 Cyg A.....	201091	8085	K5 V	5.2	1.17	0.65	2.83	4325
61 Cyg B.....	201092	8086	K7 V	6.0	1.37	0.83	3.30	3850
Gl 488.....	111631	...	M0 V	8.5	1.40	0.90	3.63	3700
Gl 570B.....	131976	5568B	M1 V	8.1	1.50	1.18	4.15	3600

TABLE 3—Continued

Name	HD	HR	Sp. Type	$V$	$(B-V)$	$(R-I)$	$(V-K)$	$T_{\text{eff}}$
GI 400A .....	...	...	M2 V	9.3	1.40	...	...	3600
GI 205 .....	...	...	M1.5 V	7.9	1.47	1.14	4.15	3400
GI 411 .....	...	...	M2 V	7.5	1.51	1.22	4.16	3350
GI 393 .....	...	...	M2 V	9.6	1.52	1.25	4.29	3325
GI 251 .....	...	...	M3 V	9.9	1.59	1.42	4.53	3250
GI 273 .....	...	...	M3.5 V	9.9	1.56	1.55	4.99	3175

comparison-star  $T_{\text{eff}}$  values differ from those given in previous papers.

### 2.3. Spectral Fitting Technique

For more details on our procedure, refer to O'Neal et al. (1998a, hereafter Paper IV; 2001). To model each active star spectrum, we used from three to seven different nonspot comparison stars and a set of spot comparison stars spanning the entire temperature range ( $3000 \text{ K} \leq T_S \leq 4000 \text{ K}$ ) over which the TiO-band technique is valid. Each possible pair of comparison stars was used to fit the active star spectrum, and an  $f_S$  was computed assuming those two temperature components. For each nonspot comparison star used (i.e., each assumed  $T_Q$ ), we plotted the relation between each assumed  $T_S$  and the resultant  $f_S$  for both the 7055 and 8860 Å bands (shown for each star in the bottom panels of Figs. 3, 5, and 7–9 below). The two relations intersect at a certain  $T_S$  and  $f_S$  (the exact point is judged using third-order best-fit polynomials). Finally,  $T_S$  and  $f_S$  values for each nonspot comparison star were averaged to derive the final, stated value of these quantities for the active star observation. Because we average fits using different proxies, we do not choose a single “best” nonspot or spot proxy for a given active star.

Both statistical and systematic uncertainties arise in our technique for deriving  $T_S$  and  $f_S$ . To estimate statistical uncertainties, we used the variance in the residuals (in plots such as those in the bottom panels of Figs. 3, 5, and 7–9) between the data points and best-fit polynomials as  $\sigma(f_S)$  values for both the 7055 and 8860 Å  $f_S$  measurements. For instance, for the DM UMa observation shown below in Figure 3,  $\sigma(f_S)$  was 0.022 and 0.033 for the 7055 and 8860 Å fits, respectively. We then plotted new “error” curves, each one an amount  $\sigma(f_S)$  above and below the actual curve. These error curves (for the 7055 and 8860 Å bands) then intersected in four points, nearly the corners of a rectangle tilted with respect to the coordinate axes. The extreme values of  $T_S$  and  $f_S$  in this “box” then yielded our statistical uncertainties in the two quantities for an observation of a particular star. (For EK Dra, since there is no constraint from the 8860 Å TiO band, we assumed for this purpose an uncertainty in  $T_S$  that was the mean of its values for the other stars.)

For systematic uncertainties, we use the rms deviation of different  $f_S$  and  $T_S$  values yielded by fitting the same active star spectrum with different nonspot proxies (all with  $T_{\text{eff}}$  within  $\sim 150 \text{ K}$  of the  $T_Q$  of the active star). Systematic uncertainties for  $f_S$  are roughly twice as large as statistical ones; for  $T_S$ , systematic and statistical uncertainties are comparable in magnitude. Assuming that systematic and statistical uncertainties are uncorrelated, we add them in quadrature to get the uncertainty values we state in § 3 for each star and in Tables 1 and 2.

In Figure 2, a plot of  $f_S$  versus phase for DM UMa, IN Vir, and EK Dra, the error bars reflect only the statistical uncer-

ainties. It is permissible to use only statistical uncertainties to judge rotational modulation because in all cases the systematic uncertainties are predictable: a given nonspot proxy, if it, e.g., yields  $f_S$  0.05 higher than fits using another nonspot proxy, will yield  $f_S$  higher by approximately that amount for every spectrum fitted. Thus, for judging rotational modulation in  $f_S$ , it is sufficient to know the uncertainty from fitting an active star spectrum with only one given nonspot proxy and to keep in mind the caveat that the *absolute*  $f_S$  values could increase or decrease as a group.

## 3. RESULTS

### 3.1. DM Ursae Majoris

From photometry, Kimble et al. (1981) found a total starspot coverage on DM UMa of at least 16% and perhaps as much as 33%, depending upon the inclination. Mohin & Raveendran (1992) found  $T_Q = 4750 \text{ K}$  and  $T_S = 3400 \pm 60 \text{ K}$  in a photometric study, while Hatzes (1995) derived  $T_Q = 4500 \text{ K}$  and  $T_S = 3300 \text{ K}$  from Doppler imaging.

This star bears a resemblance to II Peg in period (7.5 days, compared with 6.7 days for II Peg),  $v \sin i$ , spectral type, and nature as a single-lined spectroscopic binary. We thus observed

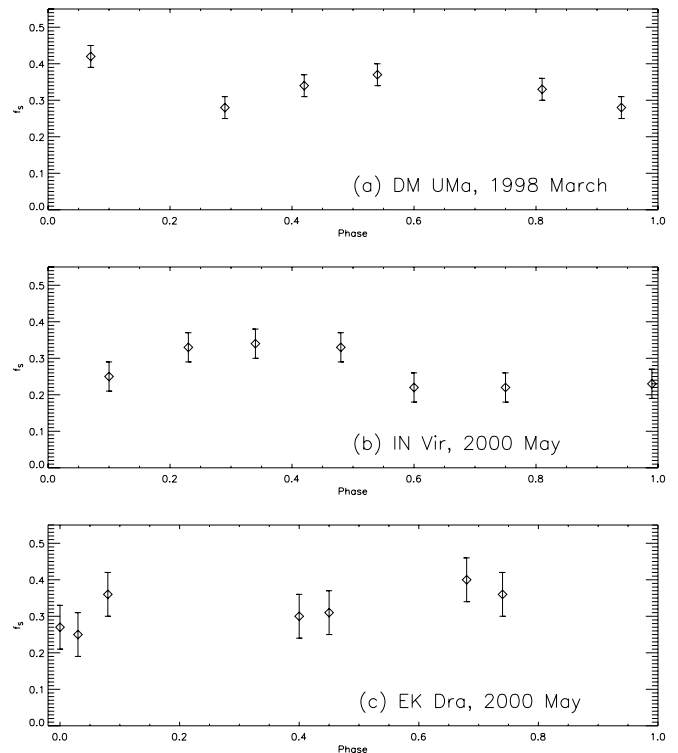


FIG. 2.—Spot filling factor vs. phase of observation for (a) DM UMa in 1998 March, (b) IN Vir in 2000 May, and (c) EK Dra in 2000 May.

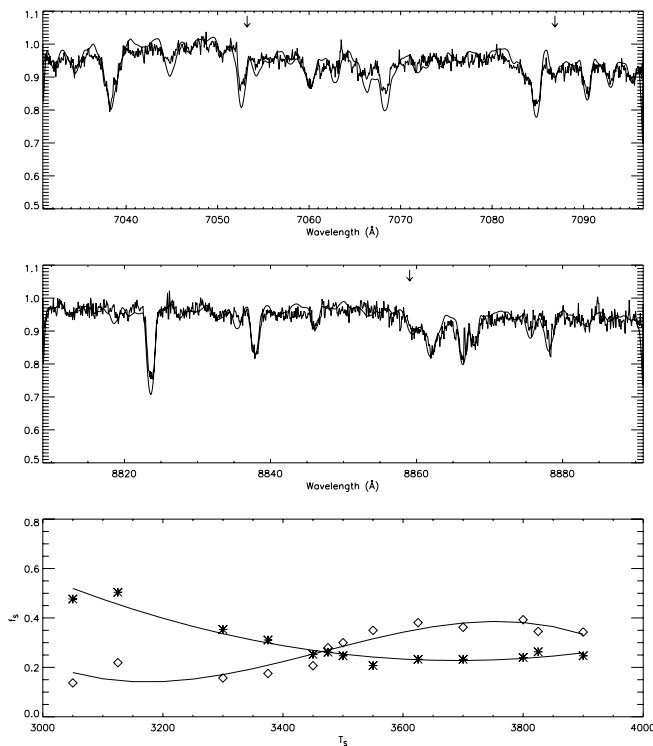


FIG. 3.—*Top*: Observed spectrum of DM UMa on 1998 March 17 in the region of the 7055 Å TiO band. A fit to the spectrum using 58 Leo as the nonspot proxy and FS Com as the spot proxy is superposed; positions of TiO bandheads (as seen in the FS Com spectrum) are marked with arrows. The fit is the smoother line (because applying a rotational broadening function smooths out noise). *Middle*: Same as above, but for the 8860 Å band in a DM UMa spectrum. *Bottom*: Illustration of the method by which fitting the 7055 and 8860 Å TiO bands of an active star (here, DM UMa) constrains  $f_S$  and  $T_S$ . For one nonspot comparison star (58 Leo), the asterisks represent  $f_S$  values obtained assuming each given  $T_S$  in fits to the 7055 Å bands. Diamonds represent the same for the 8860 Å band. The crossing point of the two relations gives  $f_S$  and  $T_S$  for DM UMa during that observation. The spectrum fitted is that of 1998 March 17.

it as a first test of whether the multiple  $T_S$  we observed on II Peg and correlations with chromospheric emission (Paper III) hold for other active stars. We obtained good phase coverage of DM UMa throughout a rotation in 1998 March. Our derived  $f_S$  are plotted in Figure 2a; these values (between 0.28 and 0.42) are similar to those reported for this star in Paper IV.

We derived  $T_S$  and  $f_S$  values by averaging fits using three luminosity class III nonspot proxies with  $T_{\text{eff}} = 4600, 4525,$  and  $4450$  K. Example fits to a DM UMa spectrum are shown in Figure 3. We detected a change of  $f_S$  as the star rotates, with a minimum of 0.28 of the visible hemisphere covered. Values of  $T_S$  on different nights of observation ranged from 3400 to 3475 K. Uncertainties are  $\pm 0.06$  for  $f_S$  and  $\pm 126$  K for  $T_S$ .

We detected enhanced  $H\alpha$  emission (presumably due either to an extended prominence [e.g., Hall & Ramsey 1994] or a flare) on 17 March (2.81 Å equivalent width, compared with an average 2.17 Å on other nights). No simultaneous enhancement was seen in the Ca II IRT lines, nor was the strength of  $H\alpha$  emission generally correlated with higher  $f_S$  or a change in  $T_S$ .

The peak of  $H\alpha$  emission was usually blueshifted with respect to the center of  $H\alpha$  absorption (in an inactive star spectrum) by  $\sim 0.5$  Å, but the enhanced emission on 17 March was centered at the same wavelength as the absorption (Fig. 4). In general, the subtracted profiles do not show the same asymmetries as the unsubtracted profiles.

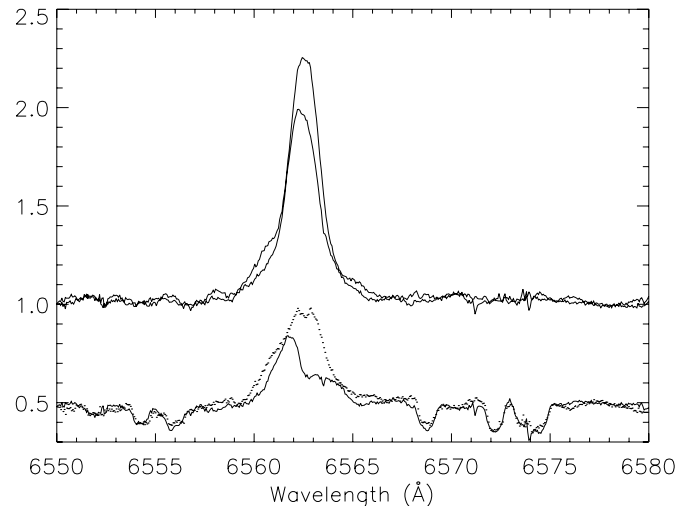


FIG. 4.—Difference in  $H\alpha$  profiles of DM UMa on two consecutive nights of observation. The original profiles are at bottom; the spectrum of 1998 March 17 is dotted, while that of 1998 March 18 is a solid line. (They are normalized so that the continuum level is 1 and then vertically offset.) The profiles after subtraction of the comparison star 58 Leo are at top.

It is possible for the  $H\alpha$  equivalent width to change even if its intrinsic flux is constant, if the level of the continuum changes. It is unlikely that this explains the difference between the two profiles in Figure 4, however. From 17 to 18 March,  $f_S$  decreased from 0.33 to 0.28. This would make the continuum  $\sim 5\%$  brighter (using appropriate values of  $T_S$ ,  $T_Q$ , and  $R_i$ ), which is not sufficient to account for the magnitude of the enhancement on 17 March.

### 3.2. IN Virginis = HD 116544

This K2–3 IV star with an 8.2 day period displays very strong Ca II emission and an inverse P Cygni  $H\alpha$  line profile. Strassmeier (1997) presented a Doppler image of this star, finding  $T_Q = 4600 \pm 70$  K and a large polar spot 1000 K cooler than the photosphere.

Averaging fits using two subgiant nonspot comparison stars ( $\gamma^2$  Del and  $\kappa$  Lyr), we found, in seven nights of observation in 2000 May, values of  $T_S$  ranging from 3275 to 3425 K. Values of  $f_S$  over the rotational cycle we observed are plotted in Figure 2b. Typical uncertainties are  $\pm 0.08$  in  $f_S$  and  $\pm 165$  K in  $T_S$ . In Figure 5 we present fits to an IN Vir TiO spectrum in the two wave bands and our computed  $f_S$  versus  $T_S$  relations.

We present an  $H\alpha$  spectrum of IN Vir in Figure 6, both before and after subtraction of the broadened absorption profile of  $\gamma^2$  Del. For IN Vir, the residual emission profile consists of a strong narrow component, peaked at the same wavelength as the  $H\alpha$  absorption in the inactive star, combined with a broad blue-shifted emission component. The strongest total (broad plus narrow components)  $H\alpha$  emission equivalent width (an enhancement of 14% over the minimum observed) and the greatest contribution from the broad component both occurred at phase 0.34, when  $f_S$  is at maximum. Peak emission in the Ca IRT lines occurred two nights earlier (near  $\phi = 0.10$ ).

### 3.3. XX Trianguli = HD 12545

XX Tri has exhibited the “largest starspot ever observed” (Strassmeier 1999). Although during week-long observing runs we were unable to obtain good phase coverage ( $P_{\text{rot}} = 24$  days), our observations characterize its spots at specific phases. The  $\Delta V$  light curve amplitude of XX Tri has been as high as 0.6 mag

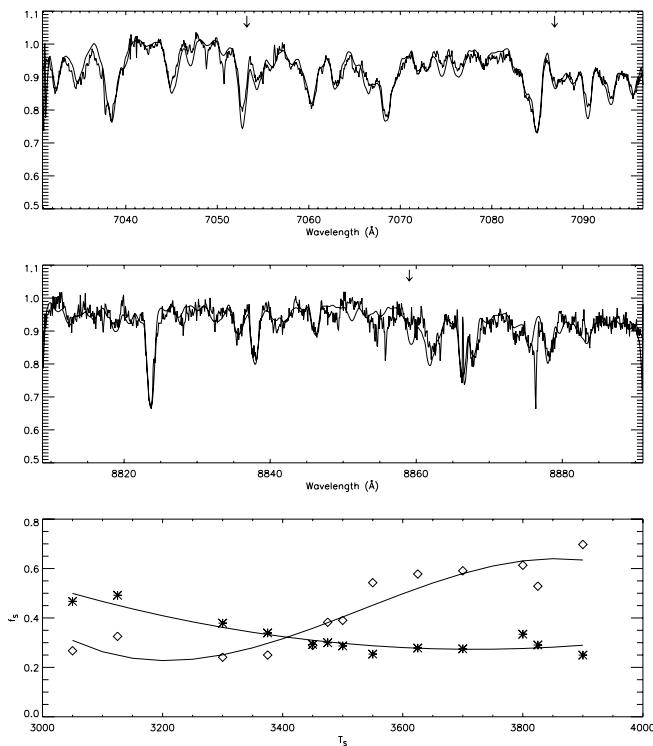


FIG. 5.—*Top and middle:* Fits to a TiO-band spectrum of IN Vir obtained 2000 May 21, using  $\kappa$  Lyr and FS Com as nonspot and spot proxies, respectively. *Bottom:* Plot of  $f_S$  vs.  $T_S$  for fits to 2000 May 21 IN Vir spectrum, with  $\gamma^2$  Del as nonspot proxy.

(Strassmeier et al. 1999). Eker (1995) found spots 1280 K cooler than a derived  $T_Q = 4820$  K, covering 27% of the star's surface. Strassmeier (1999) found a cool, high-latitude spot 1300 K cooler than  $T_Q = 4750$  K, with an area 11% of the entire stellar surface.

We observed XX Tri on 2001 December 23 and 24. With five nonspot comparison stars (luminosity class III stars with  $4675 \text{ K} \leq T_{\text{eff}} \leq 4900 \text{ K}$ ), we found  $f_S = 0.31 \pm 0.05$  and  $0.35 \pm 0.05$  for the two nights of observation and  $T_S = 3425 \pm 120 \text{ K}$  both nights (fits presented in Fig. 7). It would be of great interest to follow the TiO-band and emission-line variations of this star throughout a rotational cycle.

### 3.4. EQ Virginis = HD 118100

On this BY Dra-type flare star (K5 Ve), Saar et al. (2000) found, from TiO bands,  $T_Q = 4380 \text{ K}$ ,  $T_S = 3550 \text{ K}$ , and  $f_S = 0.43 \pm 0.05$ .

We obtained CassEchelle spectra of EQ Vir in 1998 March and 2000 May. For TiO-band fits, we used HR 5568 and 61 Cyg A as nonspot proxies (fits shown in Fig. 8). In 1998 March,  $f_S$  ranged from 0.33 (March 17) to 0.47 (March 18, 0.25 of a rotation later); in 2000 May, with better phase coverage,  $f_S$  ranged between 0.34 and 0.45. Uncertainties in  $f_S$  were  $\pm 0.07$ . We find  $T_S = 3350 \pm 115 \text{ K}$ . Emission-line equivalent widths showed no clear flares or enhancements during our observations. No current ephemeris is available for EQ Vir, so in both epochs of observation we defined our first observation to be  $\phi = 0$ .

### 3.5. EK Draconis = HD 129333

This young, single G1.5 dwarf has often been used as a proxy for the young Sun. Fröhlich et al. (2002) studied EK Dra's long-term photometric behavior, finding a secular

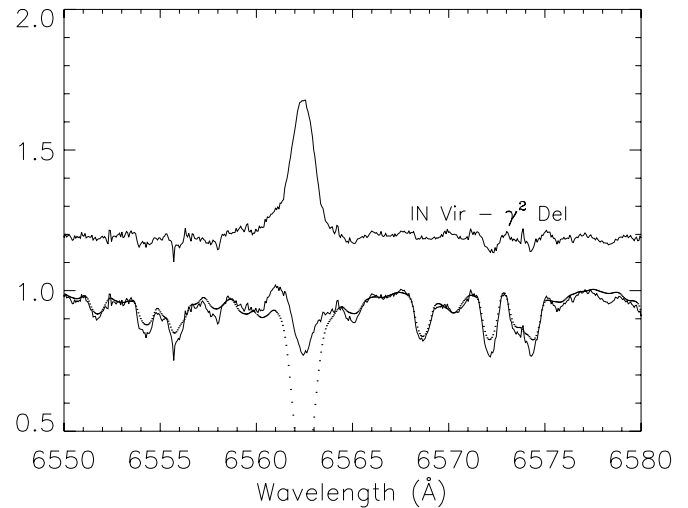


FIG. 6.—Typical  $H\alpha$  profile of IN Vir (solid line), showing the inverse P Cygni pattern. It is compared with the rotationally broadened profile of  $\gamma^2$  Del (dotted line); the difference between the two is plotted above and vertically offset. The bottom of  $\gamma^2$  Del's absorption profile is cut off to compress the plot's vertical scale.

dimming over the course of 35 yr; Messina & Guinan (2002) found a 9.2 yr cycle in its mean  $V$  magnitude and speculated that the star exhibits multiple starspot cycles. In early 2000,  $\Delta V$  was  $\sim 0.11$  mag. Its spot distribution can change significantly over a few days (Dorren & Guinan 1994).

Through light-curve modeling, Dorren & Guinan (1994) found  $T_S \sim 500 \text{ K}$  cooler than the photosphere. A Doppler image by Strassmeier & Rice (1998) yielded  $\Delta T = 1200 \text{ K}$ , compared to a 5870 K photosphere. However, we found that the

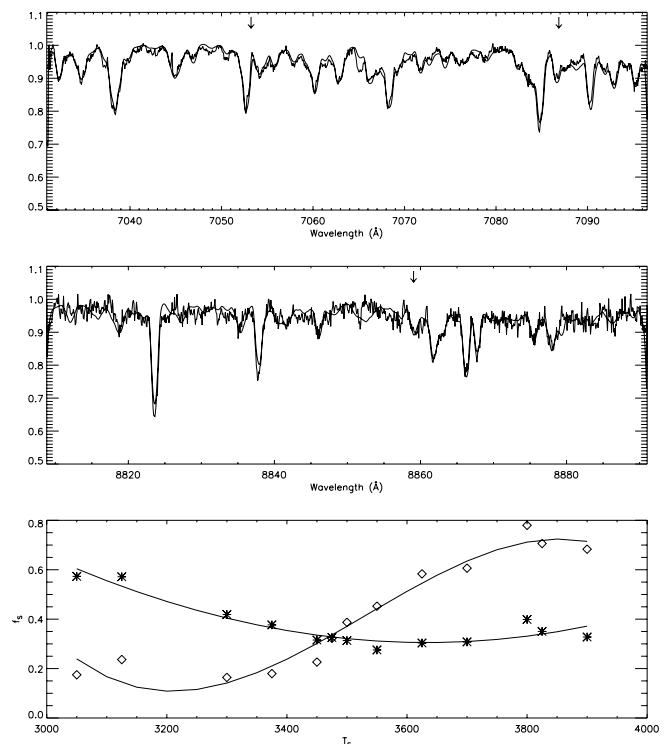


FIG. 7.—*Top and middle:* Fits to a TiO-band spectrum of XX Tri obtained 2001 December 23, using  $\theta$  Cet and BY Boo as nonspot and spot proxies, respectively. *Bottom:* Plot of  $f_S$  vs.  $T_S$  for fits to 2001 December 23 spectrum of XX Tri, using 52 Cyg as the nonspot proxy.

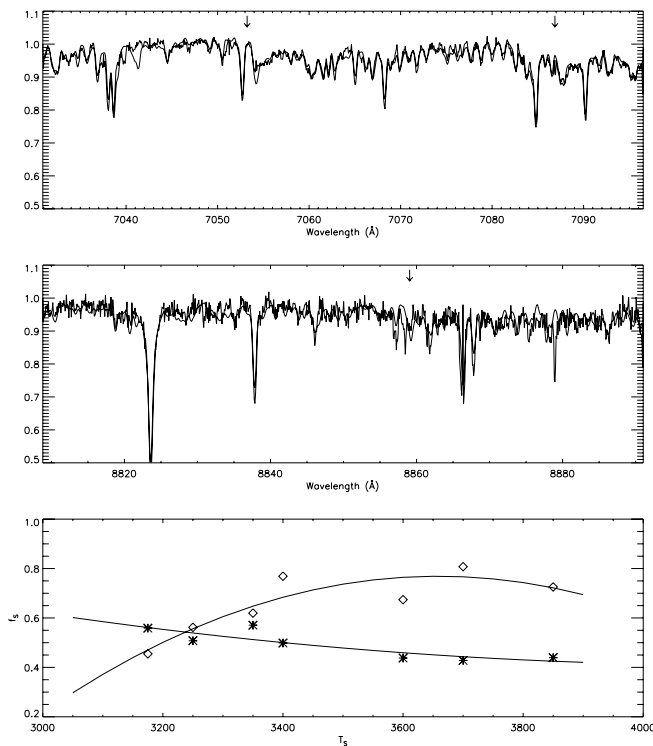


FIG. 8.—*Top and middle:* Fits to a TiO-band spectrum of EQ Vir obtained 2000 May 16, using 61 Cyg A and Gl 205 as nonspot and spot proxies, respectively. *Bottom:* Plot of  $f_S$  vs.  $T_S$  for fits to 2000 May 21 spectrum of EQ Vir, using 61 Cyg A as the nonspot proxy.

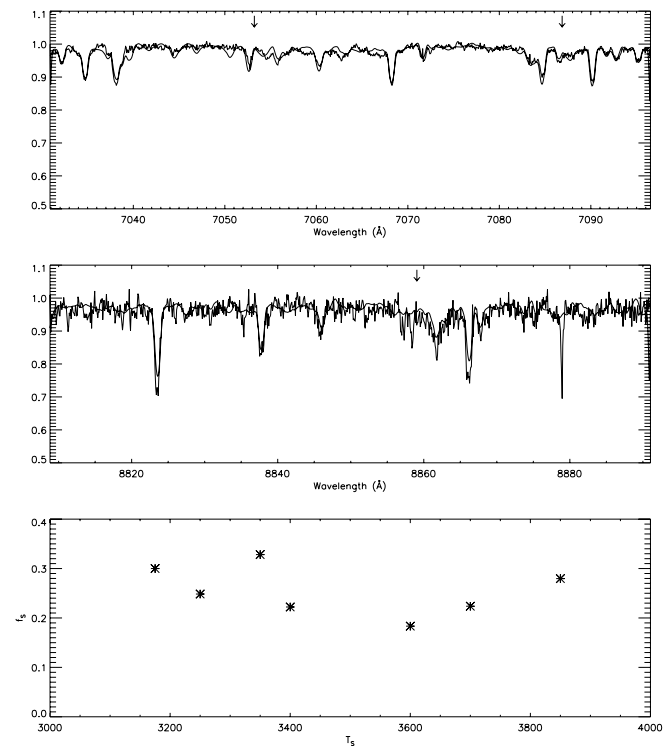


FIG. 9.—*Top and middle:* Fits to a TiO-band spectrum of EK Dra obtained 2000 May 18, using the Sun and 61 Cyg B as nonspot and spot proxies, respectively. The 8860 Å band is best fitted by assuming negligible TiO absorption, which would indicate that  $T_S \geq 3800$  K. *Bottom:* Plot of  $f_S$  vs.  $T_S$  for fits (7055 Å band only) for 2000 May 19 spectrum of EK Dra, using the Sun as the nonspot proxy.

7055 Å band was visible in our 2000 May EK Dra spectra but the 8860 Å band was not. This indicates a greater  $\Delta T$ , which would make  $T_S$  cool enough to produce TiO absorption in the 7055 Å band. In our fits (Fig. 9) we assumed  $T_S = 3800$  K (using a solar spectrum as the nonspot proxy). This lower  $T_S$  is close to typical minimum sunspot umbral temperatures, 3800–4000 K (e.g., Penn et al. 2003; Tayler 1997). We could not obtain a good fit to the 7055 Å region of EK Dra using 61 Cyg A ( $T_{\text{eff}} = 4325$  K) as a spot proxy: we obtained  $f_S \approx 0.8$ , meaning that the program tried to fit the TiO band strength with a large amount of the (very weak) TiO band in 61 Cyg A.

In Figure 2c we plot  $f_S$  as a function of phase. The photometric rotation period of EK Dra changes (Messina & Guinan 2002) and was  $\sim 2.78$ – $2.83$  days in 2000 April–May (E. Guinan 2003, private communication). Thus, instead of using a published ephemeris for EK Dra, we consider the time of our first observation to be  $\phi = 0$  (Tables 1 and 2), with  $P_{\text{rot}} = 2.805$  days.

An  $f_S$  range of 0.25–0.40 with  $T_S = 3800$  K and  $T_O = 5870$  K would produce (fluxes from Kurucz 1992 models)  $\Delta V \sim 0.22$  mag, larger than that in contemporaneous photometry. This assumes that there are no contributions to the  $V$ -band light curve other than the uniform-temperature starspots and the nonspotted photosphere. However, a recent study (Mirtorabi et al. 2003) cast doubt on whether TiO band strength and  $V$  magnitude are always so simply correlated. For the RS CVn star  $\lambda$  And, TiO variations showed many different relations to the light curve over several years, indicating significant contributions from changing bright photospheric regions.

#### 4. DISCUSSION

In previous studies (e.g., Paper I) we commented that  $f_S$  derived from TiO-band spectroscopy often exceeded values

derived from photometric light-curve modeling and Doppler imaging techniques. More recent results from other modeling methods, however, corroborate our higher  $f_S$  values. For all three evolved stars discussed herein (DM UMa, IN Vir, and XX Tri), spot parameters from photometry and Doppler imaging are similar to ours from TiO-band observations. In addition, Marino et al. (1999) found that a spot filling factor  $\geq 0.40$  at light maximum best explains multicolor photometric data of II Peg, and from a combined photometry and TiO study, Amado & Zboril (2002) found substantial nonmodulating star-spot coverage on AB Dor.

Since there is abundant evidence for large polar spots on many highly active stars (principally found through Doppler imaging studies), we tested whether, in our two-component spectral fitting procedure, the starspot proxy should have a lower  $v \sin i$  than the nonspot proxy. This would be expected if most of the spot coverage were near the star's visible pole and thus not rotating as rapidly as the star as a whole. To test this, we computed fits to the TiO-band spectra of active stars using a smaller (as compared to the star's actual projected rotation)  $v \sin i$  value to rotationally broaden the spot proxy. For DM UMa, IN Vir, EQ Vir, and EK Dra, this procedure always produced a worse fit (rms residuals of synthetic minus observed spectrum) than did the fit using the same pair of proxies and a fully rotating spot. For XX Tri, the situation was different: in tests with cooler spot proxies ( $T_S \lesssim 3600$  K), reducing the projected rotation of the spot to  $8 \pm 2$  km s $^{-1}$  (compared with the star's  $v \sin i = 28$  km s $^{-1}$ ) produced fits with the lowest residuals (a statistically significant improvement over the fits with fully rotating spots). Strassmeier (1999) found a huge high-latitude spot on this star, most visible around phase 0.75

and shortly thereafter. Our two observations occurred near this phase (albeit 4 yr later). Thus, the TiO absorption in our two spectra perhaps was dominated by this large polar feature. For the other stars, apparently enough of the spot coverage was produced by low-latitude, longitudinally distributed features that the overall spot component is best matched by a proxy rotating as fast as the star itself.

We also attempted the converse: if the spots cover primarily low-latitude area, then the star's unspotted photosphere might have a lower  $v \sin i$  than the spots. We tested this possibility using several spectra of DM UMa, EQ Vir, and IN Vir. Constraining the  $v \sin i$  of the nonspot proxy to one-third or two-thirds of the star's actual  $v \sin i$  always produced worse fits to the active star spectra. We are still exploring these effects, and this is far from an exhaustive test; more complete models would be required to investigate them in more detail.

For the four stars discussed in this paper for which we obtained good phase coverage, we found substantial starspot coverage even at the  $f_S$  minimum (e.g., 0.28 for DM UMa). This adds to the evidence that on many (perhaps most) highly active stars, a substantial spotted area is always visible. This poses a difficulty for photometric techniques that equate maximum light with an "unspotted" magnitude. The implied longitudinally uniform component of spot coverage could consist of large spots at the pole, smaller ones distributed in over the surface of the star, or any combination of the two.

Berdyugina (2002) fitted the 7055 Å bandhead of IM Pegasi (HD 216489, K1 III) with model atmospheres. She noted that the band is blended with one arising from the CN molecule, arguing that convective dredge-up as the stars age will alter the surface C and N abundances and thereby affect the CN strength. For an unspecified CN enhancement, she found that the 7055 Å band can be fitted well with quite low  $f_S$ , consistent with Doppler imaging. Based on this, Berdyugina (2002) argued that spot analyses based on the 7055 Å band and using stellar proxies should be viewed skeptically, requiring confirmation from detailed model atmosphere calculations.

For several reasons, we believe that the general situation for TiO modeling using proxies is not as dire as Berdyugina (2002) suggests. First, the stellar proxies also contain CN bands, so errors only occur when the CN strength of the proxy differs from that of the active star. Second, C and N abundances change significantly only on the ascent of the red giant branch (Iben 1967); thus, subgiants should generally be free of major CN abundance-changing effects, with dredge-up not yet, or only just, having begun (Lambert & Ries 1981; Drake 2003). Conversely, since IM Peg is a giant, the differential abundance effect is accentuated in it relative to many RS CVn's and active dwarfs. Finally, our TiO analyses have always used at least two TiO bands: the second is typically (as here) the 8860 Å band, which is not blended with CN. Even considered alone, the 8860 Å band indicates significant  $f_S$ , especially considering it is only strong at cooler  $T_{\text{eff}}$  (compared with the 7055 Å bands). In the worst case, the CN-affected 7055 Å band can be shifted to a different  $f_S$  for a given assumed  $T_S$ , and so for example, a plot like that in the bottom panel of Figure 3 will show a different crossing point for the two curves. Using a different TiO band (other than 7055 Å) would potentially eliminate this issue; some possible substitutes are the bands near 6140 and 8430 Å (Paper IV).

In previous papers, we demonstrated that the proxy spectra must be carefully selected. Proxies with incorrect  $T_Q$  or  $T_S$ , metallicity differences between proxies and targets, abundance differences (e.g., CN due to evolution), proxies with variable properties (cooler M giants), and mismatch of  $\log g$  affect derived  $f_S$  and  $T_S$  values. The last of these,  $\log g$ , is a problem for modeling active subgiants, since inactive M IV stars do not exist. Some of these issues can be addressed by using model atmospheres in place of proxy spectra; we have begun such an effort (O'Neal et al. 2004).

Mirtorabi et al. (2003) described a multiyear study of the RS CVn star  $\lambda$  And, in which they obtained photometric measurements through narrowband Wing filters to give the depth of the TiO bands, as well as standard  $V$ -band photometry. In some observing seasons, the TiO band strength was correlated with the  $V$ -band magnitude in the expected sense, i.e., stronger TiO with fainter magnitude. In other seasons, though, the two were correlated in the opposite sense or not strongly correlated at all. This indicates the inadequacy of a model postulating only the nonspotted photosphere and cooler spots as explanation for the light curves of active stars; bright spots might contribute substantially to the  $V$  light curve, and the surfaces of highly active stars are more complex than simple two-component models would indicate. This is a mystery that deserves careful study and points to the necessity of future studies that will obtain TiO-band spectra (a more reliable indicator of band strength than narrowband photometry) strictly simultaneously with  $V$ -band (and perhaps multicolor) photometry throughout more than one rotation period of a highly active star.

## 5. SUMMARY

We have presented echelle spectral data on five highly active stars (DM UMa, IN Vir, XX Tri, EQ Vir, and EK Dra) covering the 7055 and 8860 Å TiO bands, as well as the H $\alpha$  and Ca II IRT chromospheric emission features. At minimum TiO band strength the stars still display substantial ( $f_S \gtrsim 20\%$ ) levels of starspot coverage. This adds to the evidence that on highly active stars, large spotted areas are always visible, either as polar spots or as smaller spots evenly distributed in longitude. For DM UMa, IN Vir, and XX Tri, our  $T_S$  and  $f_S$  values are in rough agreement with those found in previous studies of these stars. On EQ Vir, we find lower  $T_S$  and similar  $f_S$  to those presented by Saar et al. (2000), while for the young solar prototype EK Dra, we find  $T_S$  values more similar to the temperature of sunspot umbra than to the warmer spots found by other studies. For these five stars, we found no strong correlations between emission-line strengths and starspot parameters or evidence for variable  $T_S$  as discussed in Paper III for II Peg.

D. O. received financial support from the Faculty Development Committee of West Liberty State College and the Academic Support Committee of Allegheny College. This research was partially supported by a grant from NASA administered by the American Astronomical Society (Small Research Grants to D. O. and J. E. N.). This research made use of the SIMBAD database, operated at CDS, Strasbourg, France. We thank the anonymous referee for comments that helped us improve the manuscript.

## REFERENCES

Amado, P. J., & Zboril, M. 2002, *A&A*, 381, 517  
 Berdyugina, S. V. 2002, *Astron. Nachr.*, 323, 192  
 Bessell, M. S. 1991, *AJ*, 101, 662

Bessell, M. S., Castelli, F., & Plez, B. 1998, *A&A*, 333, 231  
 Dorren, J. D., & Guinan, E. F. 1994, *ApJ*, 428, 805  
 Drake, J. J. 2003, *ApJ*, 594, 496

- Eker, Z. 1995, *ApJ*, 445, 526
- Frey, G. J., Hall, D. S., Mattingly, P., Robb, S., Wood, J., Zeigler, K., & Grim, B. 1991, *AJ*, 102, 1813
- Fröhlich, H.-E., Tschäpe, R., Rüdiger, G., & Strassmeier, K. G. 2002, *A&A*, 391, 659
- Hall, J. C., Fulton, E. E., Huenemoerder, D. P., Welty, A. D., & Neff, J. E. 1994, *PASP*, 106, 315
- Hall, J. C., & Ramsey, L. W. 1994, *AJ*, 107, 1149
- Hatzes, A. P. 1995, *AJ*, 109, 350
- Hatzes, A. P., & Kürster, M. 1999, *A&A*, 346, 432
- Hoffleit, D., & Jaschek, C. 1982, *The Bright Star Catalogue* (4th ed.; New Haven: Yale Univ. Obs.)
- Houdashelt, M. L., Bell, R. A., & Sweigart, A. V. 2000a, *AJ*, 119, 1448
- Houdashelt, M. L., Bell, R. A., Sweigart, A. V., & Wing, R. F. 2000b, *AJ*, 119, 1424
- Huenemoerder, D. P., & Ramsey, L. W. 1987, *ApJ*, 319, 392
- Iben, I. J. 1967, *ApJ*, 147, 624
- Kimble, R. A., Kahn, S. M., & Bowyer, S. 1981, *ApJ*, 251, 585
- Kurucz, R. L. 1992, *Rev. Mex. AA*, 23, 45
- Lambert, D. L., & Ries, L. M. 1981, *ApJ*, 248, 228
- Marino, G., Rodonò, M., Leto, G., & Cutispoto, G. 1999, *A&A*, 352, 189
- McCarthy, J. K., Sandiford, B. A., Boyd, D., & Booth, J. 1993, *PASP*, 105, 881
- Messina, S., & Guinan, E. F. 2002, *A&A*, 393, 225
- Mirtorabi, M. T., Wasatonic, R., & Guinan, E. F. 2003, *AJ*, 125, 3265
- Mohin, S., & Raveendran, A. V. 1992, *A&A*, 256, 487
- Montes, D., Fernández-Figueroa, M. J., de Castro, E., & Cornide, M. 1995, *A&A*, 294, 165
- Montes, D., Fernández-Figueroa, M. J., de Castro, E., Cornide, M., Latorre, A., & Sanz-Forcada, J. 2000, *A&AS*, 146, 103
- Neff, J. E., O'Neal, D., & Saar, S. H. 1995, *ApJ*, 452, 879 (Paper I)
- O'Neal, D., Neff, J. E., & Saar, S. H. 1998a, *ApJ*, 507, 919 (Paper IV)
- O'Neal, D., Neff, J. E., Saar, S. H., & Mines, J. K. 2001, *AJ*, 122, 1954
- O'Neal, D., Saar, S. H., & Neff, J. E. 1996, *ApJ*, 463, 766 (Paper II)
- . 1998b, *ApJ*, 501, L73 (Paper III)
- O'Neal, D., Saar, S. H., Neff, J. E., & Aufdenberg, J. 2004, in *IAU Symp. 219, Stars as Suns: Activity, Evolution, and Planets*, ed. A. K. Dupree & A. O. Benz (San Francisco: ASP), in press
- Penn, M. J., Cao, W. D., Walton, S. R., Chapman, G. A., & Livingston, W. 2003, *Sol. Phys.*, 215, 87
- Ramsey, L. W., & Nations, H. L. 1980, *ApJ*, 239, L121
- Saar, S. H., Peterchev, A., O'Neal, D., & Neff, J. E. 2000, in *ASP Conf. Ser. 223, Cool Stars, Stellar Systems, and the Sun*, ed. R. J. García López, R. Rebolo, & M. R. Zapatero Osorio (San Francisco: ASP), 1057
- Stauffer, J. R., & Hartmann, L. W. 1986, *ApJS*, 61, 531
- Strassmeier, K. G. 1997, *A&A*, 319, 535
- . 1999, *A&A*, 347, 225
- . 2002, *Astron. Nachr.*, 323, 309
- Strassmeier, K. G., Hall, D. S., Fekel, F. C., & Scheck, M. 1993, *A&AS*, 100, 173
- Strassmeier, K. G., Hall, D. S., & Henry, G. W. 1994, *A&A*, 282, 535
- Strassmeier, K. G., & Rice, J. B. 1998, *A&A*, 330, 685
- Strassmeier, K. G., & Schordan, P. 2000, *Astron. Nachr.*, 321, 277
- Strassmeier, K. G., Serkowitsch, E., & Granzer, T. 1999, *A&AS*, 140, 29
- Tayler, R. J. 1997, *The Sun as a Star* (Cambridge: Cambridge Univ. Press)
- Vogt, S. S. 1979, *PASP*, 91, 616
- Vogt, S. S., Hatzes, A. P., Misch, A. A., & Kürster, M. 1999, *ApJS*, 121, 547